

## Inelastic Scattering of Iron-Capture Gamma Rays from the 7.64-MeV Level of $\text{Cd}^{112}\dagger$

K. MIN

Department of Physics, University of Virginia, Charlottesville, Virginia

(Received 25 July 1966)

In the resonant-scattering experiment of the monochromatic iron-capture gamma rays from natural cadmium, five inelastically scattered photon groups were observed in addition to the 7.64-MeV elastic group. The spectrum of the low-energy cascade photons in coincidence with the scattered photons identifies the inelastic groups to be the transitions to the low-lying levels of  $\text{Cd}^{112}$ , including the three  $2^+$  vibrational levels at 0.61, 1.29, and 1.46 MeV. Angular-distribution measurements show that the 7.64-MeV resonance level in  $\text{Cd}^{112}$  has angular momentum 1. The average elastic-scattering cross section and the branching ratio for the ground-state transitions are  $\langle\sigma_{\gamma\gamma}\rangle = 0.17 \pm 0.02$  b and  $\Gamma_0/\Gamma = 0.48 \pm 0.06$ , respectively. Using these values, the self-absorption measurements determined the ground-state transition width to be  $\Gamma_0 = 0.6_{-0.1}^{+0.2}$  eV.

### INTRODUCTION

IN the last few years, the neutron-capture gamma rays have been successfully used to study the highly excited nuclear levels near the neutron binding energy by the method of nuclear resonant scattering. In comparison with a conventional gamma-ray source, such as the bremsstrahlung from the electron accelerators, the capture gamma rays are extremely monochromatic, their energies being defined within a few electron volts essentially due to the thermal motion of the capture nuclei. This monochromaticity of the capture gamma rays makes it possible to study the properties of the individual nuclear levels. Even though the probability of a given capture gamma ray satisfying the resonance condition for a particular energy level might seem small, about 50 cases of nuclear fluorescence have now been observed.<sup>1-3</sup> It is interesting to note that almost all of these cases were observed near the closed-shell nuclei, indicating a strong shell effect of the photon-transition strengths.

Giannini *et al.*<sup>3</sup> recently reported the resonant scattering of the iron-capture gamma rays from a 7.64-MeV level in natural cadmium. From the complex spectrum of the scattered gamma rays, inelastic scatterings involving 6.45- and 5.78-MeV transitions were suggested in addition to the 7.64-MeV elastic scattering.

The present work was undertaken to establish the inelastic scattering from the 7.64-MeV level by observing the low-energy cascade gamma rays and to relate them to the known level structure of the cadmium isotopes.

### EXPERIMENTAL PROCEDURE

#### A. Production of the Iron-Capture Gamma Rays

The neutron source was provided by the University of Virginia 1 MW swimming pool reactor. The experi-

mental arrangements are shown in Fig. 1. In order to reduce the fission gamma rays, which were the main source of the background in this experiment, a 1-in.-thick bismuth plate was placed next to the reactor core. The capture gamma-ray source was about one kilogram of iron placed next to the bismuth plate. The capture gamma rays then passed through a boron polyethylene filter  $1\frac{1}{2}$  in. thick and 20 in. of graphite beam hardener. An array of lead rings placed along the beam direction collimated the beam to 2 in. in diameter at the target position. With these arrangements, no appreciable neutrons were detected near the target position. An important feature of the particular configuration shown in Fig. 1 was that the target was not able to "see" the reactor core directly, and the background radiations from the core were minimized. Figure 2 shows the spectrum of the iron-capture gamma radiation  $\text{Fe}^{56}(n,\gamma)$  taken with a 5- by 4-in. NaI detector at the scattering-target position, directly facing the beam.

#### B. Scattering Arrangements

The scattering target was a natural-cadmium plate of thickness 2.5 cm. It was placed along the beam direction 2 m away from the shielding wall. The scattered photons were detected by a 5- by 4-in. NaI

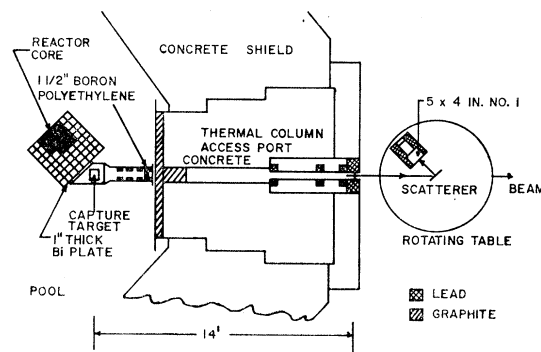


FIG. 1. Experimental arrangements.

<sup>†</sup> Supported by the National Science Foundation.

<sup>1</sup> C. S. Young and D. J. Donahue, Phys. Rev. **132**, 1724 (1963).

<sup>2</sup> B. Arad (Huebschmann), G. Ben-David (Davis), I. Pelah, and Y. Schlesinger, Phys. Rev. **133**, 684 (1964).

<sup>3</sup> M. Giannini *et al.*, Nuovo Cimento **34**, 1116 (1964).

spectrometer placed on a rotating table, with its axis of rotation fixed at the scattering-target position, and its spectrum recorded in a 400-channel R.I.D.L. pulse-height analyzer. In the normal scattering runs, with and without an absorber placed in front of the scatterer, the scatterer-to-detector distance was 20 cm. During the angular-distribution measurements, the detector was moved back to 52 cm from the scatterer, obtaining an angular resolution of 14°.

Because of the steeply rising background in the low-energy region, any low-energy cascade photons below 3 MeV which might follow the inelastically scattered photons were completely obscured in the singles spectrum (see Fig. 3). Therefore, coincidence measurements were made in which an additional 3- by 3-in. NaI

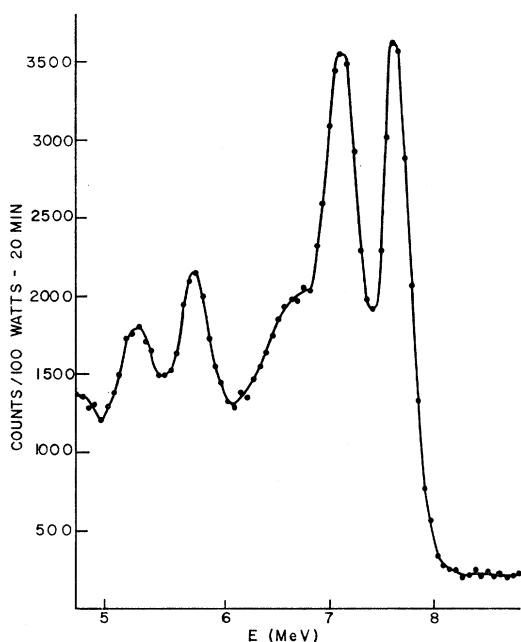


FIG. 2. Direct spectrum of iron-capture gamma radiation.

crystal looked for the low-energy cascade photons in coincidence with the inelastically scattered photons detected by the 5- by 4-in. crystal. In this measurement, the face of the target was oriented perpendicular to the incident beam, and the two detectors were placed symmetrically about the beam direction, both at 135°, with the target-detector distance of 14 cm. A slow-fast coincidence circuit was used with the resolving time  $2\tau = 40$  nsec.

During the long runs, the intensity of the incident gamma rays was frequently checked with a thimble-type ionization chamber. Throughout the experiment, the fluctuation of the beam intensity was estimated to be within 3%.

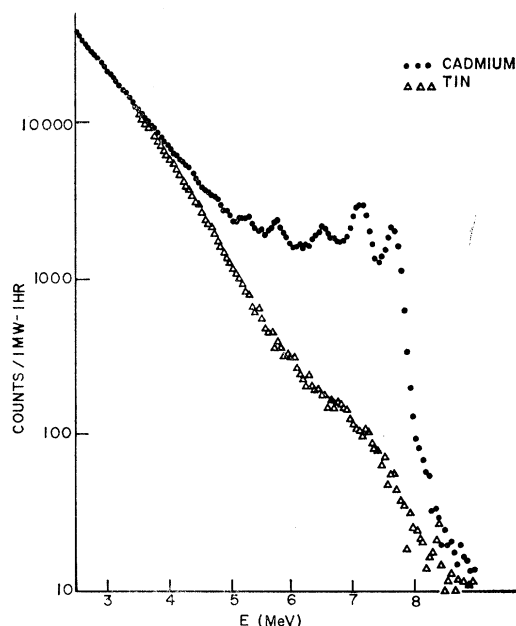


FIG. 3. Spectrum of photons scattered from natural cadmium.

## RESULTS AND DISCUSSION

### A. Spectrum of the Scattered Photons

The spectrum of the scattered photons from cadmium at the scattering angle 135° is shown in Fig. 3. The background due to the nonresonant processes indicated by the triangles was determined by replacing the cadmium target with a comparison target of tin with matched electronic absorption. The net scattering spectrum after the background subtraction is shown in Fig. 4. The expected scattering of a monochromatic-photon group is shown by the dashed line A. This response function was determined by an auxiliary scattering run from the known 7.28-MeV level in Pb<sup>208</sup>. It is evident that the scattered-photon spectrum contains several inelastic photon groups besides the 7.64-MeV elastic group. The solid line through the experimental points is the superposition of the six photon groups, marked A to F and each indicated by the dashed lines. The energies and the relative intensities of these groups are given in Table I. The uncer-

TABLE I. Energies and relative intensities of the elastic- and inelastic-photon groups. The third column gives the energy of the low-lying level populated by the given inelastic-photon group.

Component	Energy $E$ (MeV)	$7.64 - E$ (MeV)	Relative intensity (%)
A	7.64	0.00	$48 \pm 6$
B	7.03	0.61	$12 \pm 2$
C	6.35	1.29	} $9 \pm 2$
D	6.18	1.46	
E	5.78	1.86	
F	4.78	2.86	

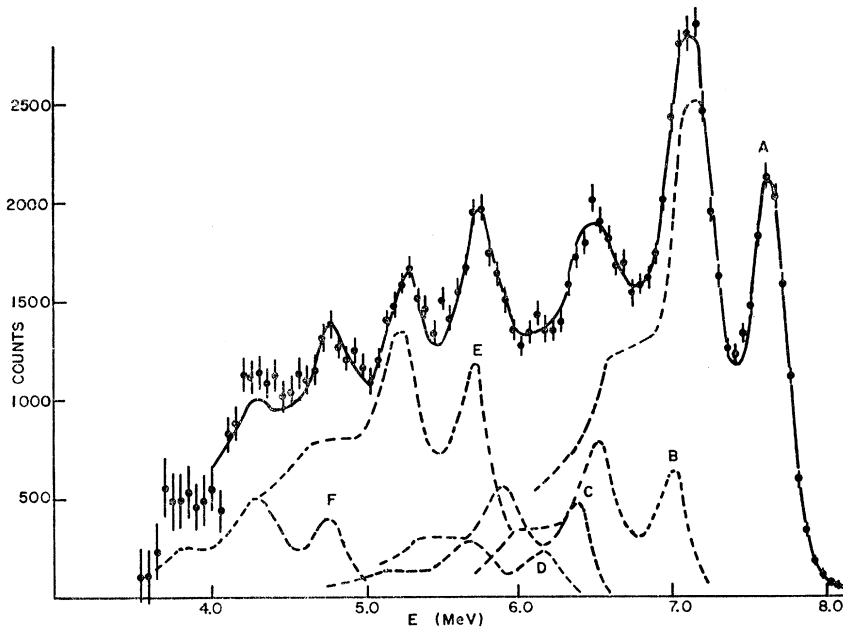


FIG. 4. Decomposition of the scattered-photon spectrum after the background subtraction. The solid line is the sum of the six components A to F which are indicated by the dashed lines.

tainty of the energy assignment is 50 keV. The relative intensity was determined by the counts under the total area of each response curve, and was corrected for the energy dependence of the total intrinsic efficiency. In the third column, the energy of each group is subtracted from the highest energy, 7.64 MeV. This would correspond to the energy of the lower level to which the 7.64-MeV level decays by the given transition.

It was noted that these energies are very close to the known excitation energies of low-lying levels of  $\text{Cd}^{112}$ . In particular, the values 0.61, 1.29, and 1.46 MeV are in good agreement with the energies of the  $2^+$  vibrational levels at 0.610, 1.295, and 1.455 MeV, observed in a Coulomb-excitation experiment.<sup>4</sup> The energy differences of 1.86 and 2.86 MeV are close to the excitation energies of 1.86 and 2.83 MeV of the two  $0^+$  levels observed in the  $\text{Cd}^{111}(d,p)\text{Cd}^{112}$  reaction.<sup>5</sup>

### B. Coincidence Spectrum of Low-Energy Photons

In order to establish the level identification mentioned above, coincidence measurements were made to search for the cascade photons from the lower levels (the third column, Table I) populated by the inelastic groups B, C, D, E, and F. Because the coincidence-counting rates were generally low, it was not practical to gate the 5- by 4-in. crystal over the individual photopeak of each inelastic group. Also, as may be seen in Fig. 4, there was an appreciable overlap between the neighboring inelastic components, due to the presence of the escape peaks and the long low-energy tail in the response of each component, which made the complete separation of each component difficult. The

"E" discriminator of the single-channel analyzer on the side of the larger crystal was set to accept the pulses corresponding to photons of energy above 6.2 MeV and 4 MeV, respectively. The coincidence spectra of the cascade photons are shown in Figs. 5(a) and 5(b). The intense peak at 0.51 MeV, which appears in both spectra, is made up exclusively of accidental and background coincidences due to the presence of large numbers of annihilation gammas in the target and the detectors. That this peak is not due to a level in cadmium was checked by taking a background coincidence spectrum, replacing the cadmium with the tin target. The result of these measurements is indicated by the solid line in Figs. 5(a) and 5(b) normalized at the valley between the 0.51-MeV and the 0.61-MeV peaks. The uncertainties in energy in Figs. 5(a) and 5(b) are about 10 keV. In Fig. 5(a), there appears only one prominent peak at  $(0.61 \pm 0.01)$  MeV, in good agreement with the energy  $(0.61 \pm 0.05)$  MeV given in Table I. The low-lying levels of the most abundant even-even cadmium isotopes are well known from Coulomb-excitation studies.<sup>4</sup> The first excited states are all known to be the first  $2^+$  vibrational states at 0.66 MeV ( $\text{Cd}^{110}$ ), 0.61 MeV ( $\text{Cd}^{112}$ ), and 0.56 MeV ( $\text{Cd}^{114}$ ). The 0.61-MeV peak in Fig. 5(a) indicates that the 7.64-MeV level belongs to the 24% abundant  $\text{Cd}^{112}$ , and that the inelastic group B populates the 0.61-MeV level in the same isotope. In Fig. 5(b), there appear four coincidence peaks at 0.61, 0.70, 0.85, and 1.24 MeV. The intensity of the 0.61-MeV peak is much larger than in Fig. 5(a), indicating that some 0.61-MeV transitions are also involved with inelastic groups other than B. According to Table I, groups C and D populate levels at 1.29 MeV and 1.46 MeV, respectively. These

<sup>4</sup> P. H. Stelson and F. K. McGowan, Phys. Rev. **121**, 209 (1961).

<sup>5</sup> B. L. Cohen and R. E. Price, Phys. Rev. **118**, 1582 (1960).

energies are in good agreement with the excitation energies of the known 2<sup>+</sup> vibrational states at 1.295 and 1.455 MeV, which are known to decay predominantly in cascades. The appearance of 0.70- and 0.85-

MeV peaks in Fig. 5(b) further supports the identification of the 1.29- and 1.46-MeV levels with the two 2<sup>+</sup> vibrational levels, in that 0.61+0.70=1.31 MeV (compared with 1.29 MeV from Table I) and 0.61+0.85=1.46 MeV (compared with 1.46 MeV from Table I). The 0.70- and 0.85-MeV peaks observed in this experiment should be compared with the 0.685- and 0.845-MeV peaks observed in the Coulomb-excitation studies of Cd<sup>112</sup>.<sup>4</sup> Figure 5(b) shows little evidence for cross-over transitions of 1.29 and 1.46 MeV. The prominent peak at (1.24±0.01) MeV may originate either from the 1.86-MeV level, populated by group E, or from the 2.86-MeV level, populated by group F. While the second possibility cannot be completely eliminated, it may be stated that the intensity of the 1.24-MeV peak is consistent with the transition from the 1.86-MeV level to the first 2<sup>+</sup> level at 0.61 MeV. The 1.86-MeV level observed in this experiment may be the 0<sup>+</sup> level observed at the same energy in Cd<sup>111</sup>(*d,p*)Cd<sup>112</sup>.<sup>5</sup> Also, the Ag<sup>112</sup> decay studies<sup>6</sup> indicate the presence of a level at 1.84 MeV which decays to the first 2<sup>+</sup> state by emitting 1.21-MeV photons. The 2.86-MeV level populated by the weakest inelastic group F may be the 2.83-MeV level observed both in the (*d,p*) and Ag<sup>112</sup> decay studies, which decays to the ground state and the first and second 2<sup>+</sup> states. If these two levels were identical, the 0.61- and 0.70-MeV peaks in Fig. 5(b) would contain some contributions due to the decay of the 2.86-MeV level.

A level scheme of Cd<sup>112</sup> and the involved photon transitions which are consistent with the spectra shown in Figs. 4, 5(a), and 5(b) are given in Fig. 6. The energies on the left-hand side are those determined in this experiment. For comparison, the level energies and

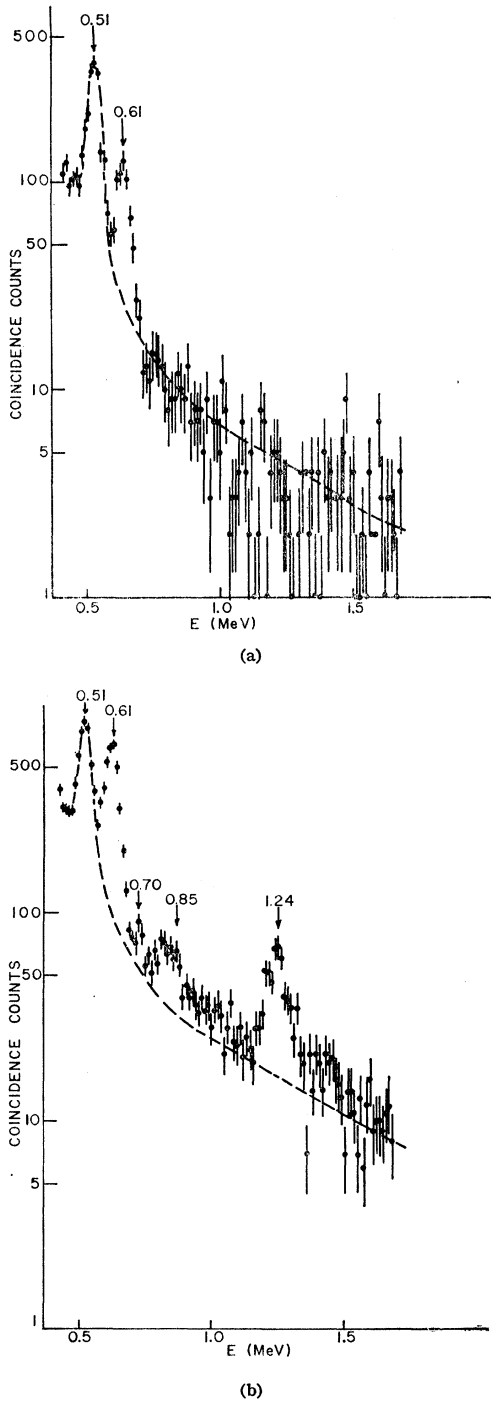


FIG. 5. (a) Spectrum of cascade photons in coincidence with the scattered photons of energy above 6.2 MeV. (b) Spectrum of cascade photons in coincidence with the scattered photons of energy above 4 MeV.

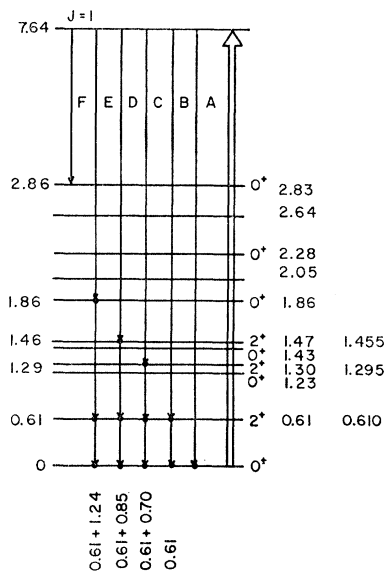


FIG. 6. Energy levels and photon transitions in Cd<sup>112</sup> observed in this experiment. For comparison, the angular momenta and energies determined in (*d,p*) (Ref. 5) and Coulomb excitation (Ref. 4) are given on the right.

<sup>6</sup> P. K. Gargis and R. van Lieshout, Physica 25, 1200 (1959).

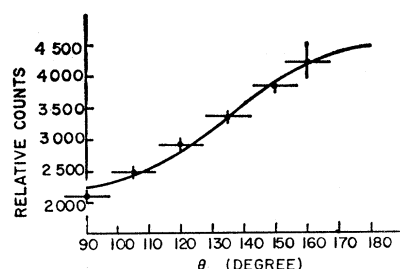


FIG. 7. Angular distribution of the elastically scattered photons. The solid line is the theoretical curve for spin 1,  $1 + \cos^2\theta$ , normalized at the  $135^\circ$  experimental point.

angular momenta determined in  $\text{Cd}^{111}(d,p)\text{Cd}^{112}$  are given on the right-hand side. The additional energies for the three lowest levels are those observed in Coulomb excitation. At the bottom, the low-energy photons in cascade with the transitions A to E are shown. The assignment of angular-momentum unity to the 7.64-MeV level is discussed below.

### C. Angular Distribution of the Elastically Scattered Photons

For the elastic peak A, the angular-distribution measurements were made at six angles. The result is shown in Fig. 7. The solid line drawn is the theoretical curve  $1 + \cos^2\theta$  for a  $0(1)1(1)0$  transition, normalized at the  $135^\circ$  point. From the good fit to the  $1 + \cos^2\theta$  distribution, it must be concluded that the 7.64-MeV level has angular-momentum unity. The possibility of two units of angular momentum of this level can be excluded, because the  $0(2)2(2)0$  angular distribution  $1 - 3 \cos^2\theta + 4 \cos^4\theta$  has a pronounced minimum about  $130^\circ$ , and it is not possible to fit this distribution through the experimental points.

### D. Self-Absorption Ratio of the 7.64-MeV Transition

If the net scattering counts with a cadmium absorber of thickness  $T$  cm placed in front of the scatterer is denoted by  $C(T)$ , the self-absorption ratio  $R$  is defined by  $R = [C(0) - e^{-\sigma_e n' T} \times C(T)] / C(0)$ , where  $\sigma_e$  is the total electronic absorption cross section and  $n'$  is the number density of the absorber atoms. The factor  $e^{-\sigma_e n' T}$  eliminates the electronic contribution to the total absorption, and the ratio  $R$  refers to the nuclear resonant absorption only. The measured quantities were  $[C(0)e^{-\sigma_e n' T} - C(T)]$ , and  $C(0)e^{-\sigma_e n' T}$ . The first quantity was taken to be the difference between counting rates of the following combinations: [Cd scatterer + Sn absorber] - [Cd scatterer + Cd absorber], in which the resonant Cd absorber and the nonresonant Sn absorber were matched in the electronic absorption. Similarly,  $C(0)e^{-\sigma_e n' T}$  was taken to be the difference [Cd scatterer + Sn absorber] - [Sn scatterer + Sn absorber]. Two absorbers of thickness 1.25 and 2.50 cm yielded  $R = (6.6 \pm 1.3)$  and  $(5.0 \pm 0.9)\%$  per cm, respectively. The absorption was taken to be the average of these two values;

$$R = (5.8 \pm 0.8)\% \text{ per cm.} \quad (1)$$

### E. Elastic Scattering Cross Section

The differential elastic scattering cross section at  $135^\circ$  was calculated using the integrated counts under the response curve A in the energy interval 6–8 MeV in Fig. 4 and the direct spectrum of the iron-capture gamma radiation shown in Fig. 2. However, in the energy interval 6–8 MeV, the iron-capture gamma radiation is known to contain admixtures of 7.28-, 6.40-, and 6.02-MeV lines<sup>7</sup> in addition to the 7.64-MeV line, which are not resolved in the NaI spectrum. Also, the 7.64-MeV line has recently been established to be a doublet of equal intensities.<sup>8</sup> The intensity of the 7.64-MeV line was obtained using the direct spectrum and the average of the two available values of the relative intensity<sup>7</sup> of the 7.64-MeV line,  $I_{7.64} / (I_{7.64} + I_{7.28} + I_{6.40} + I_{6.02}) = (74.4 \pm 4.8)\%$ . Based on the evidence presented in Sec. B that the resonant scattering is from the 24% abundant  $\text{Cd}^{112}$ , one obtains

$$\left\langle \left( \frac{d\sigma_{\gamma\gamma}}{d\Omega} \right)_{135^\circ} \right\rangle = (15.2 \pm 3.0) \text{ mb/sr}$$

for the differential cross section averaged over the incident photon spectrum. The total elastic scattering cross section was obtained using this value and taking into account the angular distribution determined in Sec. B. For the angular distribution  $W(\theta) = 1 + \cos^2\theta$ , the total elastic scattering cross section is 11.2 times the  $135^\circ$  differential cross section. Thus

$$\langle \sigma_{\gamma\gamma} \rangle = 0.17 \pm 0.03 \text{ b.} \quad (2)$$

### F. Branching Ratios for the Decay of the 7.64-MeV Level

In order to evaluate the branching ratios, the relative intensities measured at  $135^\circ$  (Table I) must be corrected for the angular distributions of the photon groups A to F. Even though the angular distribution was measured only for the elastic group A, the angular momenta of the lower levels which are populated by the inelastic groups are known from other experiments to be either  $2^+$  or  $0^+$  (Fig. 6). Therefore, the angular distribution of the groups B, C, and D must be given by  $0(1)1(1)2$  and of groups E and F by  $0(1)1(1)0$ , all with the form  $W(\theta) = 1 + a \cos^2\theta$ . The total cross section is then related to the  $135^\circ$  differential cross section by a multiplicative factor  $4\pi(1 + \frac{1}{3}a) / (1 + \frac{1}{2}a)$ , which is  $4\pi \times 0.988$  and  $4\pi \times 0.889$ , respectively, for the  $0(1)1(1)2$  and  $0(1)1(1)0$  distributions. The corrected branching ratios are practically equal to the relative intensities given in Table I (which would be the branching ratios if an isotropic distribution were assumed for all radiations),

<sup>7</sup> L. V. Groshev *et al.*, *Atlas of Gamma Ray Spectra from Radiative Capture of Thermal Neutrons* (Pergamon Press, Inc., New York, 1959).

<sup>8</sup> G. T. Ewan and A. J. Tavendale, *Nucl. Instr. Methods* **26**, 182 (1964).

being 47%, 13%, 10%, 24%, and 6%, respectively, for groups A to F. In any case, the 135° spectrum on which Table I is based was taken with a 5-in. diam crystal at 20 cm from the target, subtending a rather large angle of 38°, and the angular correlation effect discussed above is expected to have been attenuated to an appreciable extent. For the evaluation of the radiation width to be discussed below, the branching ratio for the ground-state transition was taken from Table I:

$$\Gamma_0/\Gamma = (48 \pm 6)\% \quad (3)$$

### G. Radiation Width for the Ground-State Transition $\Gamma_0$

From the measured self-absorption ratio, the elastic scattering cross section, and the branching ratio given in (1), (2), and (3) above, the radiation width for the ground state  $\Gamma_0$  can be computed if the shapes of the incident capture gamma ray and the resonant line are known.  $\Gamma_0$  was first computed assuming a pure Doppler form both for the incident radiation and the absorption line. The first assumption has been shown to be generally valid for thermal neutron-capture gamma radiation.<sup>9</sup> The assumption of the Doppler form for the absorption line, however, must be examined in terms of the ratio  $\Gamma/\Delta_s$ , where  $\Gamma$  is the total radiation width and  $\Delta_s$  is the Doppler width defined by  $\Delta_s = E(2kT/M_s c^2)^{1/2}$  ( $E$ =gamma-ray energy,  $T$ =the effective temperature of the scattering target,  $M_s$ =the mass of the scattering nuclei). In the pure Doppler approximation, it can be shown that<sup>2</sup>

$$\langle \sigma_{\gamma\gamma} \rangle = g\pi^{3/2}\lambda^2\Gamma_0 \left( \frac{\Gamma_0}{\Gamma} \right) \frac{1}{(\Delta_e^2 + \Delta_s^2)^{1/2}} \exp \left[ -\frac{\delta^2}{\Delta_e^2 + \Delta_s^2} \right],$$

$$R = ng\pi^{3/2}\lambda^2\Gamma_0 \left( \frac{1}{\Delta_s} \right) \left( \frac{\Delta_e^2 + \Delta_s^2}{2\Delta_e^2 + \Delta_s^2} \right)^{1/2} \times \exp \left[ -\frac{\delta^2\Delta_s^2}{(2\Delta_e^2 + \Delta_s^2)(\Delta_e^2 + \Delta_s^2)} \right],$$

where  $n$  is the number density of resonant nuclei;  $\Delta_e$  is the Doppler width for the capture target nuclei;  $g$  equals  $(2J+1)/(2J_0+1)$ , where  $J_0$  is the ground-state spin and  $J$  is the spin of the resonant level both in the scattering target;  $\delta$  equals  $|E_r - E_e|$ , the energy difference between the peak energies in the scatterer and the capture target nuclei. Using the measured

branching ratio  $\Gamma_0/\Gamma$ , these two equations involve two unknown parameters:  $\Gamma_0$  and  $\delta$ . For the 7.64-MeV level,  $g=3$ , and using the appropriate value for other parameters, the values

$$\Gamma_0 = 0.6_{-0.1}^{+0.2} \text{ eV},$$

$$\delta = 16_{-1}^{+3} \text{ eV}$$

were obtained. Since  $\Delta_s = 5.4$  eV for Cd<sup>112</sup>,  $\Gamma_0/\Delta_s \sim 0.1$ , the assumption of the Doppler form for the resonant cross section is, strictly speaking, not valid. However, within the stated errors, the values for  $\Gamma_0$  and  $\delta$  obtained using a more general formulation<sup>2,10</sup> are practically the same as the values obtained in the Doppler approximation. Our values of  $\Gamma_0$  and  $\delta$  disagree with those given by Giannini,<sup>3</sup> who obtained  $\Gamma_0 = 0.22 \pm 0.02$  eV and  $\delta \leq 1$  eV in the pure Doppler approximation under the assumption that the resonant scattering is due to Cd<sup>114</sup>.

### CONCLUSION

From a comparison of the energies of the low-lying levels of the Cd isotopes with the energies of the cascade photons following an inelastic photon scattering, it is possible to assign the 7.64-MeV resonance level to Cd<sup>112</sup>. This level has angular momentum 1, and decays to the 0<sup>+</sup> ground state with  $\Gamma_0 = 0.6_{-0.1}^{+0.2}$  eV and the branching ratio  $\Gamma_0/\Gamma = (48 \pm 6)\%$ . The energy positions of the five low-lying levels populated by the inelastic scattering agree with the level structure of Cd<sup>112</sup> known from other reactions. The observed vibrational levels decay preferentially by cascades with little evidence for cross over transitions.

The resonant scattering of the neutron capture gamma rays have now been reported<sup>2</sup> for about 50 nuclei. With the increasing reactor power now available, the inelastic scattering of monochromatic photons can provide a useful method to study the nuclear level structure in these nuclei.

### ACKNOWLEDGMENTS

I wish to thank Professor W. D. Whitehead for his continued interest in this work and for carefully reading the manuscript. I am indebted to Dr. W. Reed Johnson of the Nuclear Engineering Department for the installation of the tangential-thermal-beam port at the University of Virginia reactor, and for providing an efficient operation schedule. The Frederick Gardner Cottrell Grant from the Research Corporation is gratefully acknowledged.

<sup>9</sup> B. Arad, G. Ben-David, and Y. Schlesinger, Nucl. Phys. 56, 683 (1964).

<sup>10</sup> F. R. Metzger, Progr. Nucl. Phys. 7, 54 (1959).